

# Integrated simulation of runoff and groundwater in forest wetland watersheds

Cheng Genwei<sup>1</sup>, Yu Zhongbo<sup>\*2, 3</sup>, Li Changsheng<sup>4</sup>, Huang Yong<sup>2, 3</sup>

1. Institute of Mountain Hazards and Environment, Chinese Academy of Sciences, Chengdu 610041, P. R. China

2. State Key Laboratory of Hydrology-Water Resources and Hydraulic Engineering, Hohai University, Nanjing 210098, P. R. China

3. Department of Geoscience, University of Nevada Las Vegas, Las Vegas, NV 89154, U.S.A.

4. Institute for the Study of Earth, Oceans and Space, University of New Hampshire, Durham, NH 03824, U.S.A.

**Abstract:** A Distributed Forest Wetland Hydrologic Model (DFWHM) was constructed and used to examine water dynamics in the different climates of three different watersheds (a cold region, a sub-tropic region, and a large-scale watershed). A phenological index was used to represent the seasonal and species changes of the tree canopy while processes of snow packing, soil freezing, and snow and ice thawing were also included in the simulation. In the cold region, the simulated fall of the groundwater level in winter due to soil freezing and rise in spring due to snow and ice melting compare well with the observed data. Because the evapotranspiration and interaction of surface water and groundwater are included in the model, the modeled seasonal trend of the groundwater level in the sub-tropic region is in agreement with observations. The comparison between modeled and observed hydrographs indicates that the simulations in the large-scale watershed managed to capture the water dynamics in unsaturated and saturated zones.

**Key words:** *distributed hydrologic model; forest wetland; runoff; soil moisture; groundwater*

DOI: 10.3882/j.issn.1674-2370.2008.03.001

## 1 Introduction

Wetland ecosystems are capable of storing large amounts of organic carbon; they hold approximately 18%-20% of global carbon in the soil (Eswaran et al. 1995; Duxbury et al. 1993). Because of this, wetland carbon flux may significantly affect the carbon dioxide (CO<sub>2</sub>) content of atmosphere (Gorham 1991; Yu et al. 2003, 2006), which in turn affects the global carbon balance and water cycle. In recent decades, various studies have evaluated the impacts of water dynamics on wetland ecology and biogeochemical cycling (Verry and Boelter 1979; Yu et al. 2002, 2003), and especially on climate change due to global warming (Gorham 1991).

Wetland ecosystems are governed by the dynamics of surface water, soil moisture, and groundwater. Changes in the groundwater level control the growth and death of vegetation in wetlands. The decomposition rate of soil organic carbon (SOC) may also vary with the soil moisture. In cold regions, the snow packs and soil freezes of winter turn soil water into ice.

---

This work was supported by the Chinese Academy of Sciences Knowledge Innovation Project (Grant No. KZCX1-YW-08), the National Natural Science Foundation of China (Grant No. 50679018), and the Program for Changjiang Scholars and Innovative Research Teams in Universities (PCSIRT) (Grant No. IRT0717).

\*Corresponding author (e-mail: [zyu@hhu.edu.cn](mailto:zyu@hhu.edu.cn))

Received Aug. 3, 2008; accepted Sep. 9, 2008

The groundwater level may decrease with freezes and rise in the thawing period. In flat lands, the groundwater can flow horizontally through underground permeable layers. Traditional lumped models designed for a single site cannot deal with these kinds of water exchanges in space and time. In order to better evaluate the water budget in wetlands, several different distributed models have been developed for runoff and soil moisture calculations. The SWAT model can be used for design and construction purposes (Arnold et al. 2001), but not for groundwater simulation, because it cannot simulate the rise of the water table up to the ground surface. A model such as MODFLOW better simulates groundwater levels and groundwater flow in both vertical and horizontal directions (Restrepo et al. 1998). The FLATWOOD model was developed to simulate groundwater levels in flat coastal regions (Sun et al. 1998a, 1998b). The original version of the model used a simplified approach for the unsaturated soil zone. Based on the variable source area concept (VSAC) and characteristics of the topography defined by a distributed topographic index, Beven and Kirkby (1979) developed a semi-distributed physical model, TOPMODEL, to simulate watershed hydrologic processes (Beven and Wood 1983; Ambroise et al. 1996a, 1996b). In TOPMODEL it is assumed that areas with the same topographic index have hydrologic similarity. The structure of the model is simple and distinct, with fewer parameters than most other distributed hydrologic models. It has been used to simulate runoff generation in mountainous and hilly regions (Ambroise et al. 1996a, 1996b; Molicova et al. 1997). Some other distributed hydrologic models are DHSVM (Arola 1993; Wigmosta et al. 1994), HMS (Yu et al. 1999; Yu 2000; Yu et al. 2001; Yu et al. 2006), and WATFLOOD (Hamlin et al. 1998; McKillop et al. 1999; Soulis et al. 2000). The WATFLOOD model, which has adopted grouped hydrology units and is coupled with a remote sensing database, has an improved capability to predict short-term hydrologic response during a flood period. Different hydrologic units can be grouped based on remotely sensed land cover data, rather than averaged, in order to derive hydrological parameters.

A model structure that integrates the upper soil layer with shallow and deep groundwater is necessary to better simulate the hydrologic processes in forest wetlands in both unsaturated and saturated zones. The structure must be auto-adaptive to the change of the interface between unsaturated and saturated layers while the groundwater level is fluctuating. The model should also account for information on vegetation, soil, and topography because vegetation patterns, geomorphic change, and soil freezing play an important role in the water balance.

The objectives of this study are (1) to construct a distributed hydrologic model that can be evaluated and used to examine water dynamics in three different wetland watersheds, (2) to study interactions among runoff, soil moisture, and groundwater during periods of soil freezing and ice melting in a cold region, (3) to examine the dynamic relationship of fast exchange between streams and groundwater in a watershed with a sub-tropic climate, and (4) to assess how well the model can be used for hydrologic simulation of a large watershed. The

following sections consist of a description of study areas, a description of model structure and model input parameters, a discussion of the results, and conclusions.

## 2 Study sites

Three experimental watersheds, one in Minnesota, another in Florida, and a third in Carolina, were selected in order to evaluate responses in runoff generation and groundwater level under different climatic conditions.

The Marcell Experimental Forest Watershed (MEF) in Itasca County, Minnesota (latitude: 47.31°N, longitude: 93.28°W, elevation: 431 m above sea level), established in 1958, is a North Central Research Station of the United States Department of Agriculture (USDA) and the Forest Service. Subwatershed S-2 is a wetland watershed with an area of 33 hm<sup>2</sup> (82 acres), and was used for hydrologic simulation in this study. Land cover includes 8 hm<sup>2</sup> (20 acres) of bog and Black Spruce (*Picea mariana*) forest. The region has a continental climate, with cold winters and warm summers, with an annual precipitation of approximately 770 mm, one-third of which is snow. In winter the temperature can fall below -5°C. Soil freezing depths have been measured since 1962 by driving a pointed steel rod with a sliding weight on top through the freezing soil. Measurements have been taken in various soil types and land covers.

The Florida Gator National Forest Park Watershed (GNF) is in the southeastern United States, at latitude 29.4°N and longitude 82.2°W. Pine flatwood is the typical vegetation for this lower coastal plain geographic region. The GNF has been monitored since 1992 for a study of the hydrologic interactions between *Callitris robusta* in the wetlands and *Pinus elliotii* in the uplands. This region has a sub-tropic climate. The study area is about 0.5 km<sup>2</sup>. One hundred evenly-spaced wells were installed in the area to record the groundwater level. The annual precipitation is approximately 1500-1700 mm. The watershed consists of a mosaic of *Callitris robusta* in the wetlands and *Pinus elliotii* in the uplands. The exchange between surface runoff and groundwater is stronger during heavy rainfall events.

The North Carolina Bay Forest Park Watershed (CBF) is a wetland watershed in the Trend River Basin. The watershed has an area of 432.68 km<sup>2</sup>. Precipitation and streamflow have been measured at this site since 1988, but no groundwater data are available. This watershed is used to examine the model's performance in calculating rainfall-runoff generation in a large watershed.

## 3 DFWHM structure and development

### 3.1 DFWHM structure

The Distributed Forest Wetland Hydrologic Model (DFWHM), a conceptual model system, is designed to simulate water dynamics in a watershed. The structure is described in Figure 1. Input weather data (air temperature and precipitation) and watershed parameters (basin topography, vegetation, and soil patterns) drive the model simulation. The variables in

the system (soil water content in every cell) are driven by the water fluxes between upper and lower interfaces of soil layers. The DFWM is a continuous-time model that runs at a daily or hourly time step depending on the available input data.

The DFWM divides the watershed into equal-sized rectangle cells (computing units). For each cell, the surface coverage and ground structure are treated as homogeneous. The water balance and storage relationship are applied to each cell to calculate the water exchange flux vertically in the unsaturated zone and to model groundwater flow horizontally in the saturated zone (Figure 1).

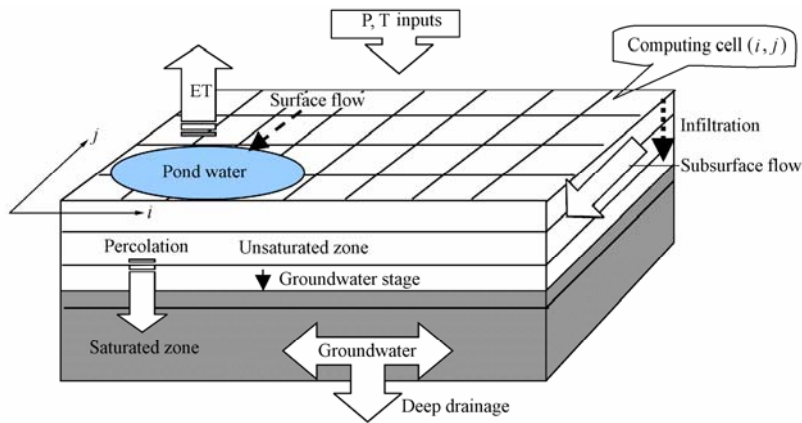


**Figure 1** Grid-layer structure of a wetland watershed  
(ET: Evapotranspiration; P: Precipitation; T: Temperature)

The DFWHM consists of five main modules: the phenology module, the forest canopy module, the surface soil layer module (which includes the litter and humus layers), the variable unsaturated soil water module, and the groundwater flow module. To facilitate examination of outputs, a graph-plotting module is designed to display the simulated results on the computer screen and to store the results in files. The water balance is computed in cells to determine the water budget at each iteration, and the groundwater exchange is conducted throughout the entire watershed to simulate the lateral groundwater exchange and the fluctuation of the groundwater level. The simulation of various processes in different modules is described in the model flow chart (Figure 2).

### 3.2 DFWM development

The DFWM has a similar structure to that of the FLATWOOD model in terms of grid system design and soil layer division (Sun et al. 1998a, 1998b). It adopts the FLATWOOD model's calculations of the phenological index ( $P_1$ ), potential and actual evapotranspiration, and canopy interception.  $P_1$  is a state variable in the model that ranges from 0 to 1 between winter and summer. It can be expressed as

$$P_1 = a + b \sin[(D_j - 91)/366] \quad (1)$$

where  $D_j$  is the serial day in a year starting on January 1, and coefficients  $a$  and  $b$  are,

respectively, 0.5 and 0.5 for hardwoods, and 0.9 and 0.1 for evergreen trees.  $P_1$  is a parameter that represents the variation of the forest watershed canopy with the season and tree species. It is used in the model to modify the calculation of vegetation transpiration and rainfall interception.

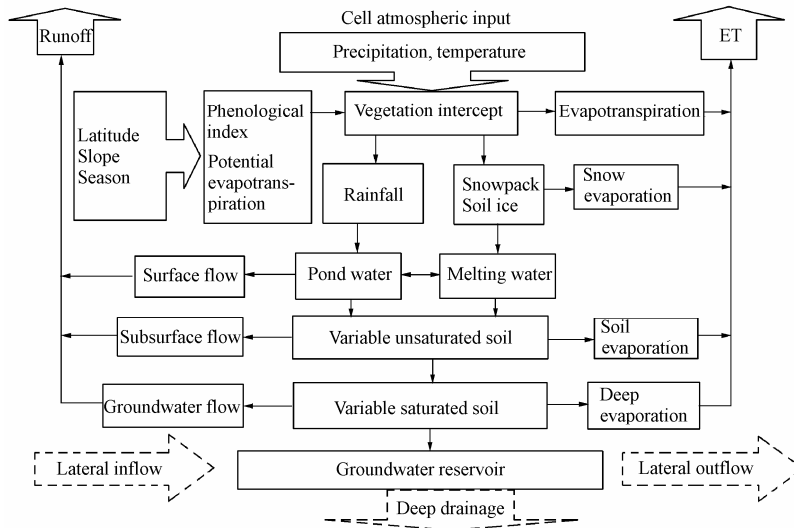


**Figure 2** Flow chart for DFWHM

Hamon's equation is used for the calculation of potential evapotranspiration ( $P_{ET}$ ):

$$P_{ET} = 0.1651L_{Day}\rho_{sat} \quad (2)$$

where  $P_{ET}$  is the daily potential evapotranspiration in mm/d,  $L_{Day}$  is the length of the day from sunrise to sunset divided by 12 hours, and  $\rho_{sat}$  is the saturated vapor density in  $g/m^3$  at the daily mean temperature ( $T_m$ ) and is calculated using the following equation:

$$\rho_{sat} = 216.7E_{sat}/(T_m + 273.3) \quad (3)$$

$$E_{sat} = 6.108\exp[17.28T_m/(T_m + 273.3)] \quad (4)$$

The interception of precipitation by vegetation ( $P_{int}$ ) is computed according to the forest pattern and season:

$$\text{Evergreen trees: } P_1 = 0.508 + 0.12P_r \quad (5)$$

$$\text{Hardwoods: } P_1 = 1.016 + 0.06P_r, \quad \text{for } t > 40 \text{ years} \quad (6)$$

$$\text{Hardwoods: } P_1 = 0.508 + 0.024P_r, \quad \text{for } t < 40 \text{ years} \quad (7)$$

$$\text{and } P_{int} = P_{IM}, \quad \text{if } P_1 > P_{IM} \quad (8)$$

$$P_{int} = P_1, \quad \text{if } P_1 < P_{IM} \quad (9)$$

where  $t$  is the tree's age, and  $P_r$  is the precipitation (mm/d) and the maximum value of interception, which varies with the date and forest pattern.  $P_{IM}$  is calculated as follows:

$$P_{IM} = P_1L_{IM} \quad (10)$$

where  $L_{IM}$  is 7.62 mm/d for conifer woods, 2.03 mm/d for hardwoods, and 1.27 mm/d for agro-grass land.

The actual evaporation calculation is applied to the water intercepted by the canopy, snow

pack on the ground surface, soil water in each layer, and groundwater. Transpiration occurs if the amount of intercepted water evaporated is less than  $P_{ET}$ . Transpiration is calculated according to the remaining  $P_{ET}$  and the vegetation coverage. The soil water is abstracted from the middle layer (a plant root depth of 30-60 cm).

A distribution function of soil water capacity has been introduced into the runoff generation module in order to improve runoff computation. This module is a key function of the Xin'anjiang Hydrologic Model, which has been widely used in flood forecasting and water resources evaluation (Zhao 1992). The surface runoff in the model is produced only when water ponds and a ground slope exists. Under those conditions, excess rainfall produces overland flow.

New methods for calculating the groundwater level and soil water infiltration, based on wetting and drying processes in the soil zone, have been used in order to improve the model's computational stability. The control equation of saturated groundwater flow in a porous medium is

$$\frac{\partial}{\partial x} \left( K_x \frac{\partial H}{\partial x} \right) + \frac{\partial}{\partial y} \left( K_y \frac{\partial H}{\partial y} \right) - Q = \mu \frac{\partial H}{\partial t} \quad (11)$$

where  $K_x$  and  $K_y$  are hydraulic conductivity along the  $x$  and  $y$  axes, respectively,  $H$  is hydraulic head,  $Q$  is a source or sink of water, and  $\mu$  is the specific yield of the porous groundwater system. In developing the model, an assumption is made that the upper soil zone (unsaturated layer) is totally empty or has a constant moisture content. Most of the time, the water content in the upper soil zone is not constant. This hydraulic equation cannot deal with variable porosity or moisture problems. To compute the groundwater level under variable upper soil moisture, the equation above is divided into two steps. The first is to calculate the flow balance between the surrounding cells and the second is to update the water level for the given cell with the net increment of change in water content. According to Darcy's Law, the flow increment  $\Delta F_x$  for cell  $(i, j)$  is, in the  $x$  direction ( $i$  coordinate),

$$\Delta F_x = A_x K_x [H(i+1) - H(i)] / [L(i+1) - L(i)] + A_x K_x [H(i-1) - H(i)] / [L(i-1) - L(i)] \quad (12)$$

and, in the  $y$  direction ( $j$  coordinate),

$$\Delta F_y = A_y K_y [H(i+1) - H(i)] / [L(i+1) - L(i)] + A_y K_y [H(i-1) - H(i)] / [L(i-1) - L(i)] \quad (13)$$

where  $A_x$  and  $A_y$  are the cross-sectional areas in the two directions and  $L(i)$  and  $L(j)$  are the coordinates on the  $i$  and  $j$  axes. The net water source for the cell is

$$S = \Delta F_x + \Delta F_y + q_{UPDRAIN} - G(t) \quad (14)$$

where  $q_{UPDRAIN}$  is the percolated water and  $G(t)$  is groundwater recharge. The groundwater level is calculated from the water balance of the interface between the saturated and unsaturated zones. The original water content in the upper soil zone (unsaturated layer) is  $W_{oi}$ .

A rise of the groundwater level is a wetting process, with soil moisture varying from  $W_{oi}$  to  $W_{sat}$ , the latter being the soil's saturation capacity, while a fall of the groundwater level is a drainage process, with soil moisture varying from  $W_{sat}$  to  $W_{field}$ , the soil's field capacity. The increment change of the water level  $D_w$  is given by

$$D_w = S / (W_{sat} - W_{oi}), \quad \text{if } S > 0 \quad (15)$$

or

$$D_w = S / (W_{sat} - W_{field}), \quad \text{if } S < 0 \quad (16)$$

The simulated water level  $S_{TG}$  for time  $t+1$  is:

$$S_{TG}(t+1) = S_{TG}(t) + D_w \quad (17)$$

## 4 DFWHM parameters

MEF and GNF experimental watersheds are divided into grid cells of 100 m by 100 m to account for the spatial distribution of vegetation. As for the CBF experimental watershed, the watershed is discretized into grid cells of 500 m by 500 m, resulting in a total number of 2925 grid cells. The model parameters can be classified into five categories: watershed dimension, evapotranspiration, freezing-thawing, runoff generation, and groundwater. These parameters are described in Table 1.

The dimension parameters of the watershed model can be obtained from the location and geometric features of a watershed. The evapotranspiration parameters ( $P_E$ ,  $E_a$ ,  $E_b$ , and  $E_c$ ) are obtained by comparing simulated and observed runoff, where  $P_E$  is the ratio of watershed evapotranspiration to the evaporation of a large water surface and  $E_a$ ,  $E_b$ , and  $E_c$  are the ratio coefficients. For instance, increasing the value of  $P_E$  will increase the computed evaporation and decrease simulated streamflow at the watershed outlet. Adjusting the  $P_E$  value within a range can improve the fit of the computed annual runoff to the amount of measured runoff. The ratio coefficients  $E_a$ ,  $E_b$ , and  $E_c$  are used in the model to account for evapotranspiration at different depths in soil layers. If the surface is bare ground or covered by short grass, most of the evapotranspiration comes from the ground surface. In that case,  $E_a$  is larger and  $E_b$  and  $E_c$  smaller. If the ground is covered with macro-phanerophytes, most evapotranspiration comes from the middle soil layer, and  $E_b$  should be larger than  $E_a$  and  $E_c$ . Thus, alternating the values of these coefficients changes the moisture distribution among the upper, middle, and lower layers in the soil profile.

The freezing and thawing parameters, freezing temperatures ( $T_s$ ,  $T_w$ ) and melting rates ( $M_s$ ,  $M_w$ ), are important to the simulation of soil freezing and thawing conditions in a cold region.  $T_s$  and  $M_s$  are the critical temperature and freezing rate of soil ice formation, respectively.  $T_w$  and  $M_w$  are the critical temperature and thawing rate of soil ice melting, respectively.  $T_s$  and  $T_w$  depend upon the difference between the temperatures of the atmosphere and the ground soil. Values range from  $-1$  to  $-3^\circ\text{C}$  for  $T_s$  and from  $+1$  to  $+2^\circ\text{C}$  for  $T_w$ .  $M_s$  and  $M_w$  range from 0.2 to 0.5 mm/( $^\circ\text{C}\cdot\text{d}$ ), fluctuating with the heat

conductivity of the soil layer.  $E_s$  is the evaporation rate of the snow surface. It has a value between 0 mm/d for a cloudy day and 0.6 mm/d for a sunny day. These parameters can be selected and optimized by comparing the simulated and observed ground freezing depths. They affect the simulated depths of snow packing and freezing soil. For warm regions, these parameters have little effect on the simulation.

**Table 1** Model parameters in the MEF, GNF and CBF

Type	Parameters	MEF	GNF	CBF	Definition
Dimension	Latitude	47.3°N	29.4°N	35.3°N	Latitude of watershed
	Delt_r	100	100	100	Cell size in row direction (m)
	Delt_c	100	100	100	Cell size in column direction (m)
	$N_{row}, N_{col}$	4, 4	4, 4	45, 65	Numbers of rows and columns of grid
	Thick1	20	20	20	Thickness of layer 1 (cm)
	Thick2	30	30	30	Thickness of layer 2 (cm)
	Thick3	50	50	50	Thickness of layer 3 (cm)
	Bottom	5	8	8	Depth of the shallow phreatic layer (computed soil depth)
Evapo-transpiration	$P_E$	1.0	1.1	1.0	Ratio of watershed evapotranspiration to the evaporation of large water surface
	$E_a$	0.2	0.3	0.3	Transpiration fraction of soil layer 1
	$E_b$	0.6	0.5	0.5	Transpiration fraction of soil layer 2
	$E_c$	0.2	0.2	0.2	Transpiration fraction of soil layer 3
Freezing	$T_s$	-1	-1	-1	Snow packing temperature (°C)
	$T_w$	-3	-2	-2	Soil frosting temperature (°C)
	$M_s$	0.8	0.6	0.6	Snow melting rate (mm/(°C·d))
	$M_w$	0.6	0.5	0.5	Soil ice thawing rate (mm/(°C·d))
	$E_s$	0.4	0.4	0.4	Snow evaporation rate, the fraction of the remains $P_{ET}$
Runoff generation	$W_{sat}$	0.45	0.40	0.40	Soil saturation capacity
	$W_{field}$	0.35	0.30	0.30	Soil field capacity
	$W_{wilt}$	0.10	0.06	0.08	Soil wilt point
	$K_{usat}$	5.5	8.0	7.0	Upper soil hydraulic conductivity at $W_{sat}$ moisture
	$K_b$	0.2	0.2	0.2	Distribution curve power index
	$C_s$	0.6	0.6	0.6	Subsurface flow storage coefficient
	$C_g$	0.95	0.95	0.98	Groundwater flow storage coefficient
	$D_m$	0.05	0.05	0.05	Shallow groundwater flow releasing coefficients
	$D_p$	0.14	0.14	0.14	Deep groundwater flow releasing coefficients
	$G_{ind}$	0.50	0.30	0.40	Groundwater flow releasing index
Ground-water flow	$K_x, K_y$	3.0	5.5	4.5	Hydraulic conductivity of saturated soil (m/d)

Surface runoff and groundwater flow are controlled by the parameters related to soil capacity ( $W_{sat}$ ,  $W_{field}$ , and  $W_{wilt}$ ), the power index ( $K_b$ ), the storage coefficient ( $C_s$ ,  $C_g$ ), and the groundwater reservoir's releasing indexes ( $D_m$ ,  $D_p$ , and  $G_{ind}$ ). The soil capacity parameters are determined through the soil texture, thickness, and slope. The larger the capacity is, the smaller the amount of simulated runoff will be. Thus, decreasing the values of  $W_{sat}$  and  $W_{field}$  will enlarge the amount of simulated runoff. The index  $K_b$  represents the heterogeneity of soil capacity in the watershed. A large value of  $K_b$  means a more homogenous soil capacity across the basin, which impacts the relationship of large and small floods. Decreasing  $K_b$  will cause the size of small floods to decrease while the size of large floods remains the same. The storage coefficients  $C_s$  and  $C_g$  influence the shape and recession rate of the hydrograph. As the value of  $C_s$  increases, the simulated subsurface flow (the main part of the hydrograph) flattens.  $C_g$  will change the shape of the hydrograph of baseflow contributed by the shallow groundwater aquifer. The ground slope and geological structure affect the returning rate of

groundwater flow (baseflow), which can be adjusted by changing parameters describing the groundwater reservoir. Increasing the values of  $D_m$  and  $D_p$  will increase the rate of groundwater returning to the river and lower the computed groundwater level.

Most model parameters are calibrated by fitting the simulated streamflow and groundwater level to the measured data. The set of parameters optimized through model calibration best reproduces hydrologic processes (generation of surface runoff, subsurface flow, groundwater flow, snow-packing, and freezing and melting of soil water) within the watershed. Meteorological data (daily precipitation and air temperature) and initial condition data (initial soil moisture and groundwater level) are used to drive hydrologic simulation of various processes. The watershed characteristics (surface elevation, land use patterns, and vegetation types) are also included in the input parameter files. The outputs of the model include variables such as evapotranspiration, soil water content, surface runoff, baseflow, and water that has infiltrated from upper soil layers to the deep aquifer, for every grid cell as well for the entire watershed. The outflow of groundwater and the fluctuation of the water table are also simulated by the model. The exchange between aquifers and streams is simulated with Darcy's Law, based on the hydraulic gradient between the two flow systems. The DFWHM was used in this study to analyze the temporal and spatial distribution of runoff generation and groundwater dynamics in response to different environmental circumstances.

## 5 Results

The model developed for this study was used in three experimental watersheds to simulate integrated surface and subsurface hydrologic components of a wetland. It was first applied in the Minnesota Marcell Experimental Forest Watershed (MEF), then in the Florida Gator National Forest Park Watershed (GNF), and then in the North Carolina Bay Forest Park Watershed (CBF).

### 5.1 Cold region

The MEF is located in the northern central United States. Because of its high latitude and elevation, the ground is covered with packed snow and frozen soil in winter. The freezing and melting of water in the upper soil layer significantly influences runoff and groundwater dynamics. The ability of DFWHM to model the soil freezing and melting processes is important in this case.

There are six subwatersheds (from S-1 to S-6) within the MEF. The forest area contains a network of rain gauges. Each subwatershed has at least two 8-inch (20.32 cm) standard rain gauges collecting data on a weekly basis. There are three recording gauges in the forest areas that provide daily values. The volume of runoff from four of the calibrated subwatersheds is measured with 120° V-notch weirs located at the catchment outlets. Elevations of the regional groundwater level at various locations in the experimental forest have been monitored since 1962. Bog subwatershed S-2 was selected for this study. Observation of precipitation and

streamflow began in 1961, while other variables (soil water content, snow packing, and soil freezing) have been observed since 1965. A total of 35 years of systematic observation data can be used in the model analysis. Surface flow, subsurface runoff, and groundwater flow were simulated in this study.

A combination of graphical and statistical methods was used to calibrate model parameters. The model's determination coefficient ( $D_c$ ) is defined as follows:

$$D_c = 1 - (\sum R_r - \sum R_s) / \sum R_s \quad (18)$$

where  $R_r$  and  $R_s$  are observed and simulated streamflow, respectively. The optimized model parameters are obtained by maximizing the determination coefficient. For the period of 1966 to 1975, the determination coefficient of the S-2 subwatershed was 0.76. For most years in the simulation period, the relative error of observed and simulated runoff was less than 15%. The simulated and observed streamflow in the MEF for the year 1966 are shown in Figure 3. The general temporal trend and magnitude of the simulated hydrographs compare well (an error of less than 10%) with the observed. The rising and descending limbs of storm hydrographs during the rainfall events were well captured.

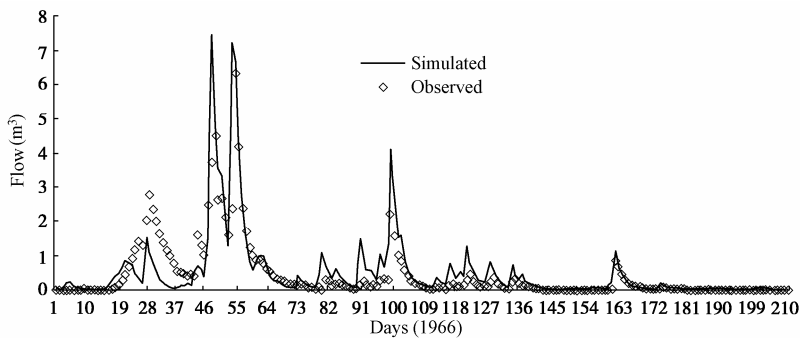


**Figure 3** Simulated and observed streamflow in the MEF

The temporal variation of simulated groundwater levels for the period of January 1, 1965 to December 31, 1966 is plotted in Figure 4, along with the observed data. The hydrograph shows a decline in the groundwater level during the winter. During the late spring, the groundwater level appears to rise along with the air temperature. This phenomenon occurred every year. Variation in the groundwater level in a cold region is caused by the freezing and thawing of soil water. The simulation shows that the soil freezes in the cold period, taking up the moisture from the upper soil layers and even from groundwater and resulting in a significant decrease in the groundwater level. In the late spring, the snow packs and soil ice melt, and water percolates to the shallow aquifer. Subsequently, groundwater rises to its highest level. This is the largest change of the groundwater level in this region. Without this module, the baseflow hydrograph of the groundwater system during these periods could not be properly captured. The results demonstrate the capability of DFWHM to simulate the variation of groundwater levels due to the freezing and melting of soil water.

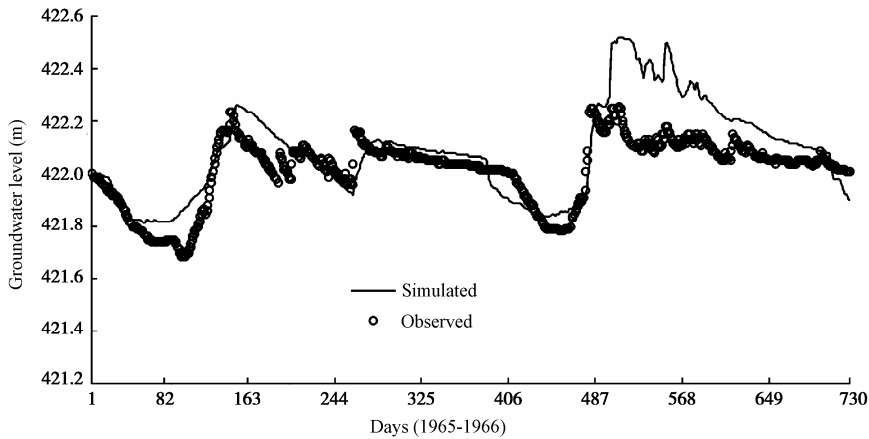


**Figure 4** Simulated and observed groundwater hydrographs in the MEF

## 5.2 Sub-tropic region

The GNF consists of a mosaic of *Callitris robusta* wetlands and forest uplands. The complex interaction between surface water and groundwater means that the groundwater level is variable and difficult to predict. The FLATWOOD model has been used in this region for wetland management and decision-making (Sun et al. 1998a, 1998b). The data set (1992-1996) calibrated in the previous study was used in this study to calibrate the DFWHM simulation. To examine the model's performance in simulating the dynamics of the groundwater flow system, two sections along the  $x$  and  $y$  directions of the basin with single and double slopes were analyzed. The ground surface and simulated groundwater level in the middle of 1992 are plotted in Figure 5. The groundwater profile fluctuates during the simulation and the hydraulic gradient in the groundwater responds to the amount and duration of rainfall via infiltration. The variation of the simulated groundwater profile in the wetland compares reasonably well with the observed data (Figure 5).

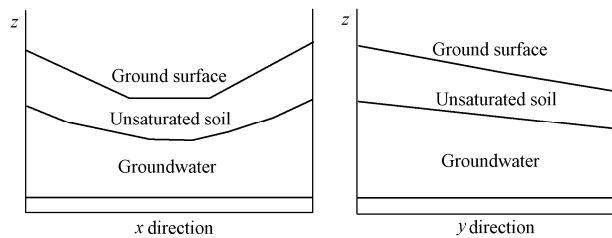


**Figure 5** Ground surface and groundwater level in the GNF

The GNF has climatic and hydrologic features that are different from the MEF. Precipitation is much higher in the GNF and the flow exchange between surface water and groundwater is intensive. For some groundwater simulation models based on groundwater hydraulic algorithms, storm rainfall inputs may produce results that diverge during the iteration computation (Sun et al. 1998a). The DFWHM does not resolve the continuous

equations of the groundwater flow system. An alternative algorithm is designed to consider wetting and drying processes in the calculation of the groundwater level. The algorithm can represent the actual processes in the soil layer.

Because of the lack of an observed streamflow data set from this watershed, a comparison can only be made between the observed and simulated groundwater levels (Figure 6). The simulated hydrograph of the groundwater level agrees with the observed one. The seasonal fluctuation of the water table was captured with the model simulation. The results show that the model can reproduce stable and reasonable response in soil moisture, runoff release, and groundwater level fluctuation.

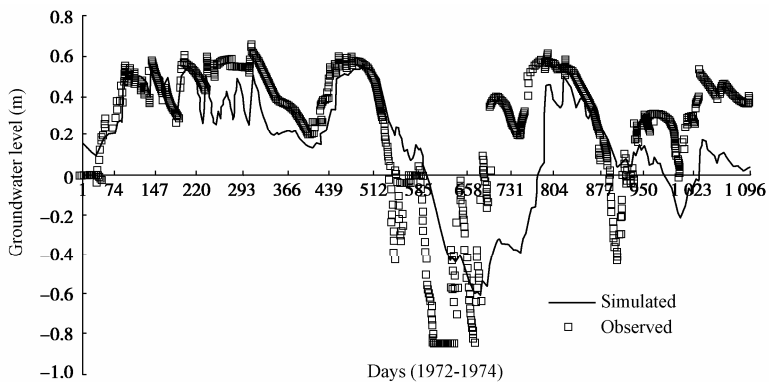


**Figure 6** Simulated and observed groundwater hydrographs in the GNF

The simulated results indicate that evapotranspiration, which is about two thirds of the annual rainfall, is the main output of the wetland (Table 2). The runoff generated in the upper soil layer is the second largest output for the entire watershed. The canopy interception of trees takes up one third of the precipitation that then turns into the evaporation. Because the wetland has a flat ground surface and a very shallow river channel, only a small amount of groundwater flows to the river. The groundwater level can rise up to the ground surface, where it pools. For these cells, the soil layers are completely saturated. Groundwater can receive recharge directly from rainfall and provide source water for evaporation to the atmosphere as well as percolation to the deep groundwater system.

### 5.3 Large watershed

The DFWHM was also applied in the CBF, a large-scale watershed with complex topography. Cell flags were used to identify the status of cells in order to account for the irregular watershed boundary. The cells within the watershed were marked with a flag of 1 and the cells outside the watershed with a flag of 0. If the cells were saturated (with ponding water, or groundwater risen to the surface), the flag was automatically marked as -1 in the simulation.

Ten years of observation data (1988-1997) are available for model parameter calibration and validation testing in the watershed. The topography of the groundwater profile within this

watershed is complex. The simulated streamflow compares well to the streamflow measured at the outlet (Figure 7, 1988). In general, high streamflow occurs early in the year and gradually decreases to its lowest point at the end of the year. The groundwater level shows a similar trend, but the highest water level arrives about one or two months later.

**Table 2** Monthly statistics of the modeled runoff and groundwater flow in the GNF

Year-month	N	Measured mean flow (mm/d)	Modeled mean flow (mm/d)	Mean difference	St. Dev. of Diff.	Total measured flow (mm)	Total modeled flow (mm)	Precipitation (mm)	AET (mm)	Interception (mm)	Soil drain flow (mm)	Groundwater (mm)
1992-01	31	0.000	0.050	-0.050	0.000	0.000	1.560	93.4	39.259	17.976	27.835	0.221
1992-02	29	0.000	0.273	-0.273	0.001	0.000	7.905	99.6	47.711	28.368	40.490	0.223
1992-03	31	0.000	1.137	-1.137	0.029	0.000	35.233	149.4	56.505	28.117	67.324	0.295
1992-04	30	0.000	1.306	-1.306	0.098	0.000	39.170	121.0	66.788	21.294	53.752	0.297
1992-05	31	0.000	0.640	-0.640	0.014	0.000	19.851	53.6	100.829	18.190	18.279	0.299
1992-06	30	0.000	2.367	-2.367	0.082	0.000	71.016	297.9	147.144	79.979	123.510	0.288
1992-07	31	0.000	1.568	-1.568	0.075	0.000	48.597	146.0	176.478	37.937	48.279	0.290
1992-08	31	0.000	0.631	-0.631	0.002	0.000	19.562	185.0	161.883	64.390	79.291	0.268
1992-09	30	0.000	0.692	-0.692	0.013	0.000	20.769	134.8	137.272	47.124	51.219	0.268
1992-10	31	0.000	2.637	-2.637	0.534	0.000	81.756	168.0	96.535	19.164	36.164	0.277
1992-11	30	0.000	0.146	-0.146	0.000	0.000	4.368	81.0	66.897	30.928	20.375	0.232
1992-12	31	0.000	0.070	-0.070	0.000	0.000	2.177	23.7	45.511	9.072	7.123	0.238
Total	366	0.000	0.960	-0.960	0.008	0.000	351.964	1553.4	1142.812	402.539	573.641	3.196

Note: N is number of days, St. Dev. of Diff. is standard deviation of difference, and AET is actual evapotranspiration.

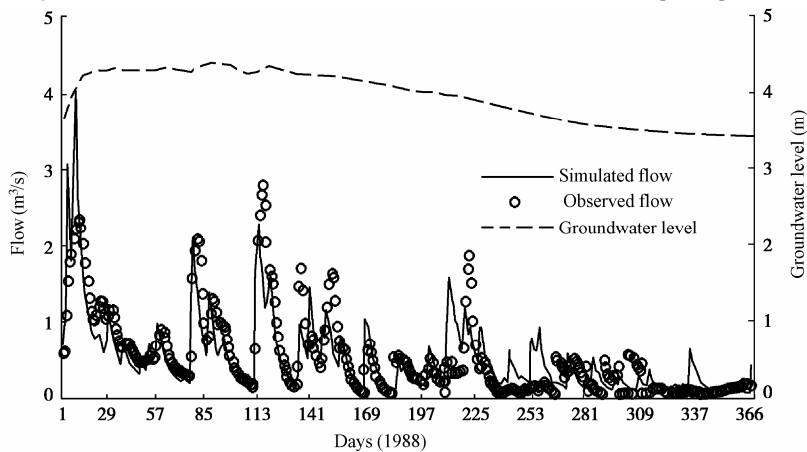


**Figure 7** The simulated and observed hydrographs in the CBF

**Table 3** Errors between measured and simulated water levels in the MEF and GNF

Regions	Average measured water table (m)	Average simulated water table (m)	Mean error	Mean absolute error	Root mean square error
MEF	422.074	422.139	-0.065	0.144	0.176
GNF	0.338	0.149	0.189	0.257	0.311

The simulated results (Table 3) show that the DFWHM can be applied to a large

watershed for hydrologic simulation. The complexity of topography does not reduce the stability of the model computation. This will be a valuable feature in future applications.

## 6 Summary and conclusions

The water budget is a crucial factor influencing vegetation growth and soil biogeochemical processes in forest wetlands. The interaction of streams and aquifers controls water distribution and dynamics within a watershed. A distributed modeling system can deal with the spatial variation in land use, vegetation cover, soil and bedrock features in these systems. In this study, the Distributed Forest Wetland Hydrologic Model (DFWHM) was developed to simulate rainfall-runoff generation and groundwater aquifer dynamics. The DFWHM is a conceptual quasi three-dimensional modeling system that discretizes the watershed into a horizontal grid with vertical layers. It is driven by precipitation and air-temperature inputs and simulates the hydrologic processes related to plant interception of precipitation, evapotranspiration, water infiltration, snow packing, and soil freezing in the watershed. A distribution curve of soil moisture capacity is introduced in the model to compute runoff on portions of the surface with a partially saturated soil layer. Groundwater levels are determined by calculating the interface of unsaturated soil layers and saturated layers.

The DFWHM was applied in a cold region, a sub-tropic region, and a large watershed. In the cold region, soil freezing is the main cause of a drop in the water table in winter, while the melting of snow and ice in the spring causes the water table to rise. If the groundwater level is high enough in places of high elevation or high latitude in winter, water will be taken up and turned into ice in the soil that may cause the water table drop. The ground slope is a key factor in the release of groundwater. If the ground surface has a small slope and the river channel is shallow, baseflow from the saturated zone is very small even if the groundwater level is high.

The comparison between simulated and observed hydrographs indicates that the model is capable of simulating watershed hydrologic dynamics in both unsaturated upper soil layers and saturated lower aquifer layers. The combined simulation of runoff and groundwater dynamics broadens our range of possibilities in studying the environment.

## References

- Ambrose, B., Beven, K., and Freer, J. 1996a. Toward a generalization of the TOPMODEL concepts: Topographic indices of hydrological similarity. *Water Resources Research*, 32(7), 2135-2145.
- Ambrose, B., Freer, J., and Beven, K. 1996b. Application of a generalized TOPMODEL to the small Ringelbach catchment, Vosges, France. *Water Resources Research*, 32(7), 2147-2159.
- Anderson, M. P., and Woessner, W. W. 1992. *Applied Groundwater Modeling: Simulation of Flow and Advective Transport*. London: Academic Press.
- Arnold, J. G., Allen, P. M., and Morgan, D. S. 2001. Hydrologic model for design and constructed wetlands. *Wetlands*, 21(2), 167-178.
- Arola, A. 1993. *Effects of the Subgrid Scale Spatial Variability on Mesoscale Snow Modeling*. M.S. Dissertation. Seattle: University of Washington.

- Beven, K. J., and Kirkby, M. J. 1979. A physically based, variable contributing area model of basin hydrology. *Hydrological Sciences Bulletin*, 24(1), 43-69.
- Beven, K. J., and Wood, E. F. 1983. Catchment geomorphology and the dynamics of runoff contributing areas. *Journal of Hydrology*, 65(1-3), 139-158.
- Duxbury, J. M., Harper, L. A., and Mosier, A. R. 1993. Contributions of agroecosystems to global climate change. In Harper, L., Duxbury, J. M., Mosier, A. R., and Rolston, D. S., eds., *Agricultural Ecosystem Effects on Trace Gases and Global Climate Change*, 1-18. Madison: American Society of Agronomy Publication No.55.
- Eswaran, H., Van den Berg, E., Reich, P., and Kimble, J. 1995. Global soil carbon resources. In Lal, R., Kimble, J. M., Levine, E., and Stewart, B. A., eds., *Soils and Global Change*, 27-43. Boca Raton: CRC Press.
- Gorham, E. 1991. Northern peatlands: Role in the carbon cycle and probable responses to climate warming. *Ecological Applications*, 1(2), 182-195.
- Hamlin, L., Pietroniro, A., Prowse, T., Soulis, R., and Kouwen, N. 1998. Application of indexed snowmelt algorithms in a northern wetland regime. *Hydrological Processes*, 12(10-11), 1641-1657.
- McKillop, R., Kouwen, N., and Soulis, E. D. 1999. Modeling the rainfall-runoff response of a headwater wetland. *Water Resources Research*, 35(4), 1165-1177.
- Molicova, H., Grimaldi, M., Bonell, M., and Hubert, P. 1997. Using TOPMODEL towards identifying and modelling the hydrological patterns within a headwater, humid, tropical catchment. *Hydrological Processes*, 11(9), 1169-1196.
- Restrepo, J. I., Montoya, A. M., and Obeysekera, J. 1998. A wetland simulation module for the MODFLOW ground water model. *Ground Water*, 36(5), 764-770.
- Soulis, E. D., Snelgrove, K. R., Kouwen, N., Seglenieks, F., and Verseghy, D. L. 2000. Towards closing the vertical water balance in Canadian atmospheric models: Coupling of the land surface scheme CLASS with the distributed hydrological model WATFLOOD. *Atmosphere-Ocean*, 38(1), 251-269.
- Sun, G., Riekerk, H., and Comerford, N. B. 1998a. Modeling the forest hydrology of wetland-upland ecosystems in Florida. *Journal of the American Water Resources Association*, 34(4), 827-841.
- Sun, G., Riekerk, H., and Comerford, N. B. 1998b. Modeling the hydrologic impacts of forest harvesting on Florida flatwoods. *Journal of the American Water Resources Association*, 34(4), 843-854.
- Verry, E. S., and Boelter, D. H. 1979. Peatland hydrology. In Greeson, P. E., Clark, J. R., and Clark, J. E., eds., *Wetland Functions and Values: The State of Our Understanding*, 389-402. Minneapolis: American Water Resources Association.
- Wigmosta, M. S., Vail, L. W., and Lettenmaier, D. P. 1994. A distributed hydrology-vegetation model for complex terrain. *Water Resources Research*, 30(6), 1665-1679.
- Yu, Z., Lakhtakia, M. N., Yarnal, B., White, R. A., Miller, D. A., Frakes, B., Barron, E. J., Duffy, C., and Schwartz, F. W. 1999. Simulating the river-basin response to atmospheric forcing by linking a mesoscale meteorological model and hydrologic model system. *Journal of Hydrology*, 218(1-2), 72-91.
- Yu, Z. 2000. Assessing the response of subgrid hydrologic processes to atmospheric forcing with a hydrologic model system. *Global and Planetary Change*, 25(1-2), 1-17.
- Yu, Z., Carlson, T. N., Barron, E. J., and Schwartz, F. W. 2001. On evaluating the spatial-temporal variation of soil moisture in the Susquehanna River Basin. *Water Resources Research*, 37(5), 1313-1326.
- Yu, Z., Barron, E. J., Yarnal, B., Lakhtakia, M. N., White, R. A., Pollard, D., and Miller, D. A. 2002. Evaluation of basin-scale hydrologic response to a multi-storm simulation. *Journal of Hydrology*, 257(1-4), 212-225.
- Yu, Z., Shangquan, X., Pollard, D., and Barron, E. J. 2003. Simulating methane emission from a Chinese rice field as influenced by fertilizer and water level. *Hydrological Processes*, 17(17), 3485-3501.
- Yu, Z., Pollard, D., and Cheng, L. 2006. On continental-scale hydrologic simulations with a coupled hydrologic model. *Journal of Hydrology*, 331(1-2), 110-124.
- Zhao, R. J. 1992. The Xinanjiang Model applied in China. *Journal of Hydrology*, 135(1/4), 371-381.